ORNL/Sub--94-SS110/02

ORLN/Sub/94-SS110/02

Corrosion Protection of SiC-Based Ceramics with CVDMullite Coatings

May 1, 1997

Report Prepared by
Vinod Sarin and Michael Auger
Boston University
Manufacturing Engineering
15 St. Mary's Street
Boston MA 02215

under
ORLN/Sub/94-SS110/02

for

OAK RIDGE NATIONAL LABORATORY
Oak Ridge, Tennessee 37831
Managed by
LOCKHEED MARTIN ENERGY RESEARCH CORP.
for the
U.S. DEPARTMENT OF ENERGY
under contract DE-AC05-96OR22464

ORLN/Sub/94-SS110/02

Corrosion Protection of SiC-Based Ceramics with CVDMullite Coatings

May 1, 1997

Report Prepared by
Vinod Sarin and Michael Auger
Boston University
Manufacturing Engineering
15 St. Mary's Street
Boston MA 02215

under
ORLN/Sub/94-SS110/02

for

OAK RIDGE NATIONAL LABORATORY
Oak Ridge, Tennessee 37831
Managed by
LOCKHEED MARTIN ENERGY RESEARCH CORP.
for the
U.S. DEPARTMENT OF ENERGY
under contract DE-AC05-96OR22464

Research sponsored by the U.S. Department of Energy, Fossil Energy Advanced Research and Technology Development Materials Program, DOE/FE AA 15 10 10 0, Work Breakdown Structure Element BU-2

Abstract

For the first time, adherent crystalline mullite coatings have been chemically vapor deposited onto SiC substrates to enhance its corrosion/oxidation resistance. Thermodynamic and kinetic considerations have been utilized to produce mullite coatings with a variety of growth rates, compositions, and morphologies. The flexibility of processing can be exploited to produce coated ceramics with properties tailored to specific applications and varied corrosive environments. These corrosive environments include thermal, Na_2SO_4, O_2, and coal slag.

Research sponsored by the U.S. Department of Energy, Fossil Energy Advanced Research and Technology Development Materials Program, DOE/FE AA 15 10 10 0, Work Breakdown Structure Element BU-2

Abstract (Insert 1st paragraph of Introduction)

For the first time, adherent crystalline mullite coatings have been chemically vapor deposited onto SiC substrates to enhance its corrosion/oxidation resistance. Thermodynamic and kinetic considerations have been utilized to produce mullite coatings with a variety of growth rates, compositions, and morphologies. The flexibility of processing can be exploited to produce coated ceramics with properties tailored to specific applications and varied corrosive environments. These corrosive environments include thermal, Na_2SO_4, O_2, and coal slag.

1

360205
360201

INTRODUCTION

Silicon carbide ceramics are the leading candidate materials for use as heat exchangers in advanced combined cycle power plants because of their unique combination of high temperature strength, high thermal conductivity, excellent thermal shock resistance, and good high temperature stability and oxidation resistance. Ceramic coatings are being considered for diesel engine cylinder liners, piston caps, valve faces and seats, piston rings, and for turbine components such as combustors, blades, stators, seals, and bearings [1]. Under such conditions ceramics are better suited to high temperature environments than metals.

Si_3N_4 and SiC are limited by their susceptibility to specific high temperature corrosive environments, including fossil fuels. These environments include but are not limited to hot gas streams containing trace amounts and combinations of impurities such as SO_x, NaCl, and O_2 [2]. Combined with the inherent liability of monolithic ceramics to contact stress failure, this corrosion resistance limitation has lead to the development of protective coatings. Innumerable coatings have been developed throughout the last seven decades yet none has met the complex internal requirements of high temperature engines [3].

Mullite has been targeted as a potential coating material for silicon based ceramics such as Si_3N_4 and SiC. In addition to traditional refractory applications, mullite has received considerable attention as a high temperature material because of its unique ability to retain its strength, resist creep, and avoid thermal shock failure at elevated temperatures [4,5,6,7]. At atmospheric pressure, mullite is the only stable crystalline compound in the Al_2O_3-SiO_2 system. Stoichiometric mullite is quoted as $3Al_2O_3 \bullet 2SiO_2$ yet exists between 57 and 74 mole% Al_2O_3. The crystal

structure of mullite is a modified defect structure of sillimanite ($Al_2O_3 \bullet SiO_2$) in which the mullite stoichiometry is achieved by substituting Si^{4+} ions with Al^{3+} ions in the tetrahedral sites and forming an oxygen vacancy [8,9]. The well accepted defect structure is expressed as $Al^{VI}_2(Al^{IV}_{2+2X}Si_{2-2x})O_{10-x}$ where x denotes the amount of missing oxygen and VI and IV denote six-fold and four-fold coordination. Stoichiometric mullite is orthorhombic and theoretically fits between sillimanite (x=0) and alumina (x=1) [10]. This full solid solution range has not been achieved in practice and mullite rarely exists beyond 76 mol% alumina with conventional processing. Solid solubility depends on the formation process and the cooling rate with extreme Al_2O_3 concentrations resulting from temperatures in excess of 2000°C and rapid cooling rates.

Previous attempts to grow mullite coatings by various processing methods have met with limited success [11]. Most commonly reported techniques require a post deposition heat treatment to convert the amorphous alumina-silicate into crystalline mullite [12,13]. Deposition of plasma sprayed mullite coatings have been reported; however, inherent porosity in the coatings resulted in migration of corrodants through the coating after a few hundred hours [14]. To overcome these deficiencies, the direct formation of chemically vapor deposited (CVD) mullite coatings has been investigated. The CVD process results in dense adherent coatings with the ability to control microstructural and morphological properties.

THERMODYNAMIC ANALYSIS

Equilibrium thermodynamics was performed on the $AlCl_3$-$SiCl_4$-CO_2-H_2 system to establish equilibrium reaction products at various operating conditions. This analysis has been detailed in previous publications [15,16]. and were used to create CVD phase diagrams that help establish guidelines for input conditions for producing mullite and other compounds at equilibrium. The overall equilibrium reaction yielding mullite from the reactant gases utilized in the CVD process is theorized to be the following:

$$6AlCl_3 + 2SiCl_4 + 13CO_2 + 13H_2 \rightarrow 3Al_2O_3 \bullet 2SiO_2 + 13CO + 26HCl \qquad (1)$$

Thermodynamic analysis was performed using a wide range of conditions including temperatures between 800 and 1200°C and system pressures between 2 and 150 torr. The results of the previous analysis determined that low concentrations of chlorides need to be used to obtain high deposition efficiency and carbon free deposits.

KINETIC CONSIDERATIONS

A comprehensive thermodynamic analysis is necessary but not sufficient for understanding the CVD process parameters required to grow mullite coatings. Analyzing the kinetic steps, in particular the rate limiting step, involved in the coating deposition is also essential. Current studies focus on collecting experimental data concerning the kinetics of CVD mullite formation using $AlCl_3$, $SiCl_4$, H_2, and CO_2. Kinetic considerations are being taken from the formation of the

well established oxide coatings Al_2O_3 and SiO_2 using chloride reactants. The formation of Al_2O_3 proceeds via this hydrolysis reaction:

$$CO_2(g) + H_2(g) \rightarrow CO(g) + H_2O(g) \quad (2.1)$$

$$2AlCl_3(g) + 3H_2O(g) \rightarrow Al_2O_3(g) + 6HCl(g) \quad (2.2)$$

It has been shown that the reaction rate of $AlCl_3$ with O_2 is extremely slow while $AlCl_3$ reacts vigorously with H_2O. $AlCl_3$, H_2, and CO_2 exhibit a moderate reaction rate and avoid homogenous nucleation [17]. The reaction proceeds via reaction (2) where reaction (2.1)is labeled the water-gas shift reaction. It has also been stated that SiO_2 is formed via the hydrolysis mechanism at 1000°C, yet it is unclear whether SiO2 can easily form via another mechanism [18].

Experimentally it has been found that the rate is proportional to the concentration of both reactants (assuming the reaction is irreversible). Hence the rate equation for H_2O production is

$$R_{H2O} = k[CO_2]^n[H_2]^m \quad (3)$$

In this equation, k is called the rate constant for this reaction. It is independent of concentration yet will vary with temperature according to the Arrhenius relation. The factors n and m refer to the rates of the equation and are not necessarily equal to the stoichiometry of the formation equation. For instance if $n = 1$ the reaction is considered first order with respect to carbon dioxide.

The water-gas shift reaction has been extensively studied due to its applicability to metal oxide reactions [19]. Analysis of the reaction over the temperature range 400 to 1050°C suggest separate low temperature and high temperature reaction paths. The low temperature reaction path is dominant at temperatures below 800°C and is extremely sensitive to trace impurities such as oxygen. The high temperature reaction is homogenous and dominant at temperatures in excess of 800°C. The respective low and high temperature mechanisms (determined by measuring CO concentration) are as follows:

$$\text{Low Temperature: } dC_{CO}/dt = 7.6\text{x}10^{4}\text{Exp}\left(\frac{-39{,}200}{RT}*\right)[H_2]^{1/3}[CO_2] \qquad (4)$$

$$\text{High Temperature: } dC_{CO}/dt = 1.2\text{x}10^{13}\text{Exp}\left(\frac{-78{,}000}{RT}*\right)[H_2]^{1/2}[CO_2] \qquad (5)$$

*activation energy is stated in cal/mole

The activation energy of SiO_2 and Al_2O_3 on Si substrates varies according to experimental conditions. Two similar studies performed in cold-walled CVD reactors state an SiO_2 activation energy of 82kcal/mol [20]. and an Al_2O_3 activation energy of 34.8kcal/mol [21]. These separate studies agree with numerous experimental observations in which Al_2O_3 deposition is particularly sensitive to trace impurities in the gas mixture resulting in homogenous (powdery) nucleation [22]. These previous kinetic studies have been used as guides for CVD mullite yet may not be used directly as the kinetics of the mixed chloride reaction will vary from the kinetics of the separate systems.

EXPERIMENTAL METHODS

A CVD reactor consisting of a vertically hot-walled reactor with a resistively heated three-zoned furnace was used for the experiments. Polished bars of 3 x 4 x 20 mm Hexaloy SiC (Carborundum Company, Niagara Falls, NY) were used as substrates. $AlCl_3$ was formed *in situ* by flowing Cl_2 with Ar as a carrier and dilutant through heated Al chips. $SiCl_4$ vapor was introduced by evaporating the liquid at room temperature. CO_2 and H_2 were mixed with the chlorides prior to entering the deposition reactor. Excess H_2 was present to ensure complete reduction of the metal chlorides to form HCl before exiting the reactor. The deposition technique is detailed in previous literature [23]. All depositions reported in this study were performed at 950°C and a total pressure of 75 torr. All coatings were characterized through x-ray diffraction (XRD) and scanning electron microscopy (SEM). Selected coatings were characterized with electron diffraction, transmission electron microscopy (TEM), and scanning transmission electron microscopy (STEM).

RESULTS AND DISCUSSION

Effect of Input Gas Stoichiometry

The effect of the input Al:Si ratio on the resultant mullite coating was investigated. The ratio of Al:Si was varied from pure SiO_2 to pure Al_2O_3 with composite coatings varying between 1:1 to 4:1. Experimentally there are numerous methods to achieve the desired input Al:Si molar ratios. The two methods explored in this study are 1) varying the total partial pressure of metallic

chlorides (P_{MClx}) by altering the flow rate of $AlCl_3$ and holding the flow rate of $SiCl_4$ constant and 2) holding P_{MClx} constant and varying both $AlCl_3$ and $SiCl_4$ to achieve the desired ratio.

The effect of varying the Al:Si ratio through varying P_{MClx} is shown in Figure 1. An initial increase in growth rate is seen as $AlCl_3$ is introduced at an Al:Si ratio of 1:1 and P_{MClx} of 0.33 torr The coatings produced at a 1:1 ratio and P_{MClx} of 0.33 torr were not usually mullite when examined through XRD and exhibited a high degree of non-uniformity. TEM analysis reveled that these coatings were a nano-crystalline mixture of γ-Al_2O_3 and amorphous SiO_2. This nano-crystalline layer was evident in all samples tested at all input ratios. Details of similar structural analysis may be found in a previous study [24]. The growth rate of the coating continues to decrease as the $AlCl_3$ flow rate is increased to an Al:Si ratio of 4:1 and P_{MClx} of 0.93 torr. The degree of homogenous nucleation (powder formation) and non-uniformity in the coating continued to increase as the Al:Si ratio increased. The surface morphology of the coating becomes more faceted as the input Al:Si ratio increases. Previous studies of CVD mullite coatings have shown that increased Al content increases the faceted nature of the coating [17]. Mullite coatings grown with an input Al:Si ratio of 2:1 were uniform, fine grained, and highly faceted with a growth rate of 3 μm/hr. The growth rate for Al_2O_3 stated in Figure 1 is an average value taken from several literature sources under similar conditions. Attempts to deposit Al_2O_3 using mullite processing conditions resulted in significant homogenous nucleation. Pure SiO_2 coatings under these conditions were found to be amorphous.

The effect of varying the Al:Si ratio by increasing P_{MClx} on the initial nano-crystalline region is shown in Figure 2. The thickness of the nano-crystalline region decreases as the input Al:Si ratio increases. Compositional analysis on the 2:1 and 3:1 samples, carried out in an STEM

using a 40nm electron probe, indicate a variation in the Al:Si ratio across the thickness of the coatings. The Al:Si ratio near the substrate is very low, a typical value is 0.326 and is presumed to be SiO_2 at the substrate coating interface. The Al:Si ratio increases as the analysis proceeds through the nano-crystalline region. The coating begins to grow as (001) textured columnar mullite at the point where the Al:Si ratio is between 2.93 and 3.77. This ratio overlaps with the known Al_2O_3 solid solubility of mullite (2.76-3.33). The Al:Si ratio continues to increase through the nano-crystalline region with maximum values approaching 7:1 at the top of the coating. The presence of a nano-crystalline region suggests that mullite is not forming directly as thermodynamics suggests but rather as Al_2O_3 and SiO_2 separately. These molecules are absorbed on the surface of the silicon-based substrate with SiO_2 initially preferred. Mullite nucleates when the Al:Si ratio of the initial nano-crystalline coating reaches a critical value close to that of stoichiometric mullite.

Figure 3 illustrates the effect of growth rate upon the second method of controlling the input Al:Si ratio by maintaining the P_{MClx} at 0.53 torr and varying both $AlCl_3$ and $SiCl_4$ to achieve the desired ratio. The constant P_{MClx} value was 0.53 torr , the same value for the 2:1 coatings grown in Figure 1. Unlike in the varying P_{MClx} matrix the coatings grown at all mixed oxide compositions were uniform, fine-grained, and faceted mullite coatings. The degree of homogenous nucleation did not visually change throughout the mixed oxide range. Growth rates of coatings with an input Al:Si ratio of 1:1, 2:1, and 4:1 did not vary significantly, however the growth rate of coatings grown at the stoichiometric mullite input ratio of 3:1 was significantly larger. Figure 4 indicates the X-ray diffraction pattern of the mullite coating grown under the Al:Si ratio of 3:1 with a P_{MClx} of 0.53 torr at 950°C and a total pressure of 75 torr

The Effects of Depletion

Depletion through deposition and homogenous nucleation in a hot-walled reactor usually results in non-uniform coatings. Excessive homogenous nucleation results in powdery non-adherent coatings. Mullite deposition has the added complexity of multiple components. In an attempt to better understand the effects of depletion upon the uniformity of CVD mullite, a 10 cm long sample of Si_3N_4 (Norton NT154) was placed parallel to input gas flow, as illustrated in Figure 5. The coated sample was sectioned and analyzed. There is a temperature gradient along the length of the sample with deposition at the bottom of the sample occurring at 930° and the deposition at the top was 980°C. Such a gradient is common in industrial CVD depositions to minimize the effects of depletion. Increased temperature is required to maintain a constant growth rate with increasingly depleted reactants. A constant growth rate was maintained along the entire length of the sample. SEM micrographs reveal that the coating becomes increasingly faceted from the bottom to the top. This is due to the increasing Al:Si ratio evident in the EDS quantitative analysis performed on each section

The Effects of Post-Deposition Thermal Treatment

Post-deposition heat treatments were conducted on SiC coated samples with coatings grown by varying P_{MClx} to achieve different Al:Si input ratios. Studies were conducted on mullite coatings grown at Al:Si input ratios of 1:1, 2:1, 3:1, and 4:1, as well as SiO_2. Separate coating sets were thermally treated in a vacuum tight chamber at atmospheric pressure in a flowing Ar environment at 1000°C for 100 hours, 1200°C for 100 hours, and 1350°C for 4 hours. The

structures of mullite coatings on SiC grown at an input Al:Si ratio of 2:1 and heat treated under these conditions are shown in Figure 6. As the temperature of the annealing treatment increased the surface structure became increasingly featureless. X-ray diffraction of the coatings after heat treatment indicated that the only crystalline phases present were mullite and SiC.

Figure 7 illustrates the surface structure of coatings produced with different input Al:Si ratios by varying the partial pressure of metallic chlorides (P_{MClx}) after annealing at 1350°C for 4 hours. The coating grown with an input Al:Si ratio of 2:1 is relatively featureless as compared to the coating grown with an input ratio of 4:1. The coatings grown with a larger Al:Si input ratio maintained their surface structure better than the coatings grown with a lesser input Al:Si input ratio. The surface structure of mullite coatings can be controlled during thermal treatments without any apparent adverse effects upon the integrity of the coating.

Grain growth did occur in the mullite coating as indicated in Figure 8 which compares the same coating before and after annealing at 1350°C. Grain growth is particularly evident in the resolution of the (120),(210) peak doublet post-anneal. Grain growth most likely occurred through the conversion of columnar mullite grains into a coarse grained and textured mullite coating.

Uncoated and amorphous SiO_2 coated SiC were subjected to elevated temperatures for comparative purposes. The X-ray diffraction patterns of Figures 9 and 10 indicate that both the native and deposited amorphous SiO_2 crystallized at elevated temperatures. The SiO_2 peak is evident in both the uncoated and initially amorphous SiO_2 coated SiC at 22° (2θ). An SiO_2

crystalline phase is not evident in mullite coated samples that have been heat treated to 1000°C, 1200°C, or 1350°C.

Corrosive Environment Studies

Preliminary experimentation has begun to determine the degree of protection provided by mullite coatings on silicon-based ceramics in corrosive environments. Different corrosive environments may require mullite coatings with slightly different properties. This degree of control may be achieved with CVD mullite coatings.

Oxidation Environment

CVD mullite coated SiC was tested in an O_2 rich environment at 1000°C for 100 hours [25]. As shown in Figure 11 an extremely low weight gain is observed past 30 hours of exposure. The extremely low weight change (little formation of oxide) is shown as the weight change versus square root of time(assuming parabolic oxide growth kinetics) for times greater than 30 hours. At this point, there is no statistical difference in the growth kinetics between mullite coated with an input Al:Si ratio of 2:1 ($P_{MClx.}$ = 0.53 torr), 3:1 ($P_{MClx.}$ of 0.53 torr), and the slow diffusion rate of O_2 through the protective SiO_2 layer that forms on SiC.

Na_2SO_4, O_2 Environment

CVD mullite coated Si_3N_4 was subjected to a corrosive environment containing Na_2SO_4 and O_2 at 1000°C for 100 hours [26]. The specimens were typically loaded with about 5 mg/cm^2 of Na_2SO_4 and exposed to a flowing oxygen environment in a quartz tube heated to 1000°C. The use of an oxygen environment results in a basic molten salt (i.e., high Na_2O activity), thus facilitating the corrosive reaction of Na_2O with native SiO_2 seen on silicon based substrates according to the reaction:

$$Na_2SO_4(l) \rightarrow Na_2O(s) + SO_3(g) \quad (6.1)$$

$$Na_2O(s) + xSiO_2(s) \rightarrow Na_2O \bullet x(SiO_2)(l) \quad (6.2)$$

The results of uncoated Si_3N_4 and mullite coated Si_3N_4 after exposure are shown in Figure 12. The presence of a Na-containing glassy phase is observed to a depth of $\approx$ 20 μm below the initial substrate surface in the uncoated sample. Yttrium (used as a sintering aid in Si_3N_4) migrated through the grain boundaries of the substrate to the substrate surface, resulting in the formation of a yttrium depleted zone of $\approx$ 10 μm. The mullite coated sample was relatively unaffected by the corrosive environment. It was found from TEM study that the remainder of the coating as well as the underlying Si_3N_4 substrate were not affected either microstructurally or compositionally by the corrosion exposure.

Coal Slag

With the desire to tailor CVD mullite coatings on ceramic heat exchangers in coal-fired systems for power production, CVD mullite coated SiC samples were exposed to corrosive coal slag at 1260°C for 300 hours [27]. Chemical composition of the coal slag is given in Table I. Corrosive coal slag will form extreme porosity and dramatic pit formation in unprotected SiC. After 300 hours of exposure all mullite coatings (Al:Si input ratios 2:1, 3:1, 4:1 achieved through varying P_{MClx}) exhibited excellent protection. Generally, mullite grown with a lower input Al:Si ratio exhibited a more corrosion resistant surface as shown in Table II. This trend agrees with the as deposited SEM analysis of mullite coatings in which an input Al:Si ratio of 2:1 (P_{MClx} 0.53 torr) produced a more uniform coating than an input Al:Si ratio of 4:1 (P_{MClx} 0.93 torr).

CONCLUSIONS

Through the use of thermodynamic and kinetic analysis crystalline mullite coatings have been deposited via chemical vapor deposition upon silicon based materials such as SiC and Si_3N_4. Altering process parameters such as deposition temperature and reactant partial pressure has resulted in mullite coatings with varied physical and chemical properties such as crystal structure, surface morphology, and chemical composition. Preliminary results have indicated that mullite coatings form an effective barrier to corrosion in high temperature corrosive environments including Na_2SO_4-O_2, oxidation, and jet burner exhaust.

ACKNOWLEDGMENTS

Research sponsored by the U.S. Department of Energy, Assistant Secretary for Energy Efficiency and Renewable Energy, Office of Transportation Technologies, as part of the Ceramic Technology Project of the Propulsion System Materials Program, and Fossil Energy AR&TD Materials Program under contract numbers DE-AC05-840R21400 and SC-19X-SS110C with Martin Marietta Energy Systems, Inc. The authors would like to acknowledge Dr. Woo Lee, Dr. Tom Strangman, and Dr. Peter Tortorelli for corrosion testing, Ping Hou for TEM analysis, Dr. S. Basu for invaluable discussions, and Dave Stinton for his guidance.

REFERENCES

1. W.J. Lackey, D.P. Stinton, et.al., *Advanced Ceram. Mat.*, **2** [1], 24-30, (1987)

2. N.S. Jacobson, *J.Am. Ceram. Soc.*, **76** [1], 3-28, (1993)

3. W.J. Lackey, D.P. Stinton, et.al., ORNL/TM-8959 (1984)

4. I.A. Aksay, D.M.Dabbs, M. Sarikaya, *J. Am. Ceram. Soc.*, **74** [10] 2343-58 (1991)

5. P.F.Becher, *J. Am. Ceram. Soc.*, **74** [2] 255-69 (1991)

6. S.Somiya, Y. Hirata, *Am. Ceram. Soc. Bull.*, **70** [10] 1624-32 (1991)

7. R.D. Nixon, S. Chevacharoenkul, R.F. Davis, and T.N. Tiegs, pp. 579-603 in Ceramic Transactions, Vol. 6, *Mullite and Mullite Matrix Composites*, Edited by S. Somiya, R.F. Davis, and J.A. Pask, American Ceramic Society, Westerville, OH, 1990

8. D.G.W. Smith and J.D.C. McConnel, *Mineral. Mag.*, **35** [274] 810-14 (1966)

9. T. Epicier, *J. Am. Ceram. Soc.*, **74** [10] 2359-66 (1991)

10. C.W. Burnham, *Carnegie Institute Washington Year Book*, **63**, 227-228, (1964)

11. J. Schienle, and J. Smyth, Final Report, ORNL/Sub/84-47992/1 (1987)

12. K. Okada, N. Otsuka, pp.425-34 in Ceramic Transactions, Vol. 6, *Mullite and Mullite Matrix Composites*, Edited by S. Somiya, R.F. Davis, and J.A. Pask, American Ceramic Society, Westerville, OH, 1990

13. O.R. Monteiro, Zhi Wang, Ian G. Brown, *J. Mat. Res.*, To be Published

14. K.N. Lee, N.S. Jacobson, R.A. Miller, *MRS Bulletin* **19** [10], 35-38, (1994)

15. R.P. Mulpuri, and V.K. Sarin, 19th Annual Cocoa Beach Conference and Exposition on Engineering Ceramics, Cocoa Beach, FL, The American Ceramic Society, Westerville, OH, (Jan. 1995)

16. R.P. Mulpuri, and V.K. Sarin, *J. Mater. Res.*, 11 (6), 1315-24, (1996)

17. Ph, Wong, M. Robinson, *J.Am Ceram. Soc.*, **53**, 617-21, (1970)

18. W.Steinmaier, J.Bloem, *J. Electro. Soc.*,**111** (2), 206-209, (1964)

19. G.L. Tingey, *J. Phy. Chem.*, **70** (5), 1406-1412, (1966)

20. W.Steinmaier, J.Bloem, *J. Electro. Soc.*,**111** (2), 206-209, (1964)

21. S.W. Choi, C. Kim, et.al., pp.233-41 in the proceedings of the IX International Conference on CVD (CVD-IX), as part of the Electrochemical Society Meeting held in Cincinnati, OH, *May 7-10, 1984*, ed. McD. Robinson, The Electrochemical Society Inc., Pennington, NJ, 1984

22. H. Altena, K. Stjernberg, B. Lux, pp. 381-90 in the proceedings of the V European Conference on CVD (Euro-CVD-V), held in Uppsala, Sweden, *June 17-20, 1985*, ed. J. - O. Carlsson, Uppsala University, Department of Chemistry, Uppsala, Sweden

23. V.K. Sarin and R.P. Mulpuri, *U.S. Pat. Pending*

24. D.Doppalaupudi, et.al., pp. 664-70 in the proceedings of the XIII Annual CVD Conference, as part of the Electrochemical Society Meeting held in Los Angeles, CA, *May 5-10*, 1996, ed. T.M.Besmann, The Electrochemical Society Inc. Pennington, NJ, 1996

25. Testing performed by Dr. Tortorelli of Oak Ridge National Laboratory, Oak Ridge, TN

26. W.Y. Lee, K.L. More,Y.W. Bae, *J. Am. Ceram. Soc.*, **79** (9), 2489, (1996)

27 Testing performed by Dr. K. Breder of Oak Ridge National Laboratory, Oak Ridge, TN. For further test information see: K. Breder, et.al., "Strength Measurements of Monolithic SiC and Al_2O_3/SiC Composites after Exposure to Coal Slag," *J. Am. Ceram. Soc.*, **78** (10), 2837-40, (1995)

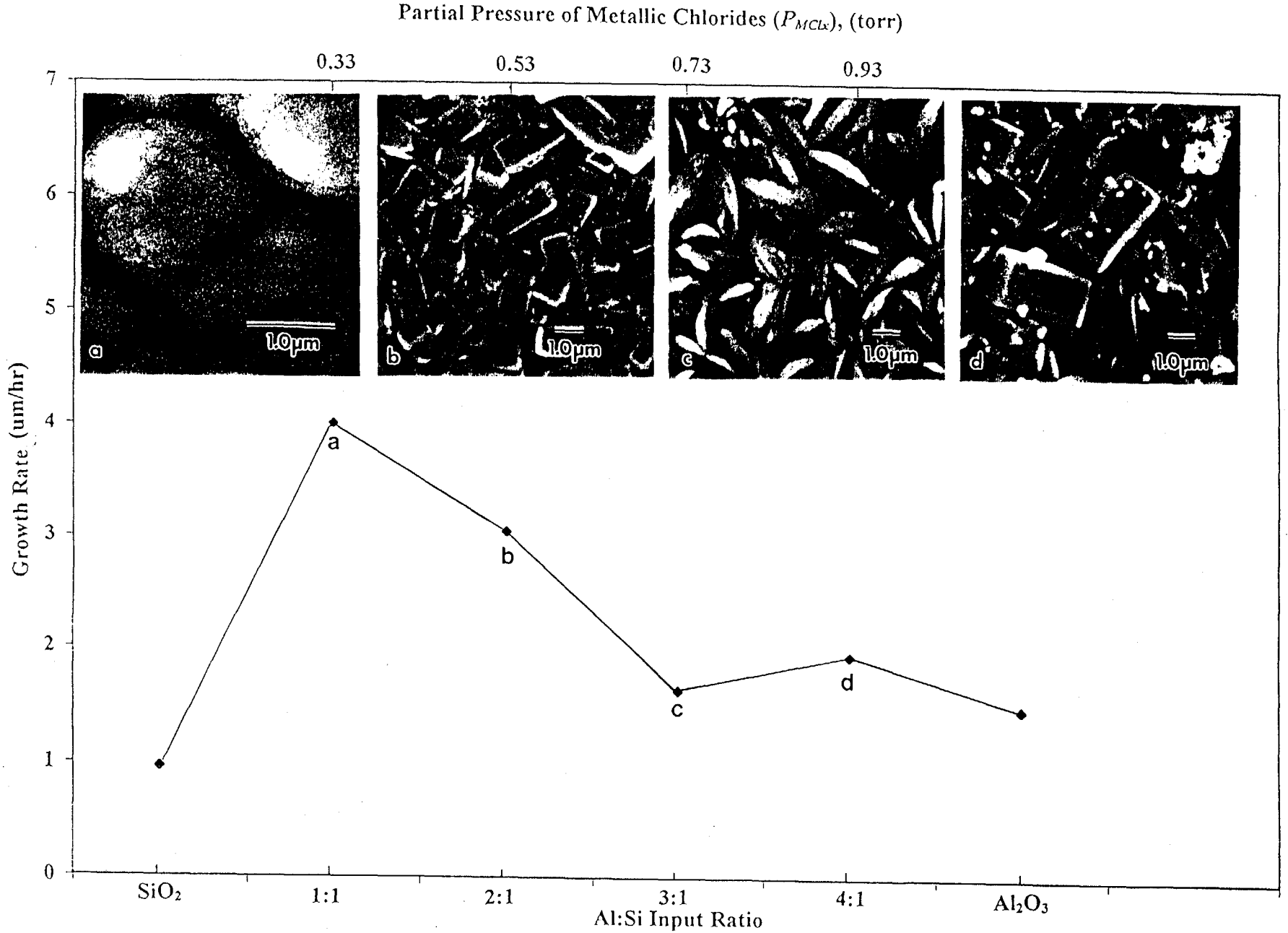

Figure 1: Growth rate of mullite vs. reactant Al:Si ratio and variable metallic chloride partial pressure

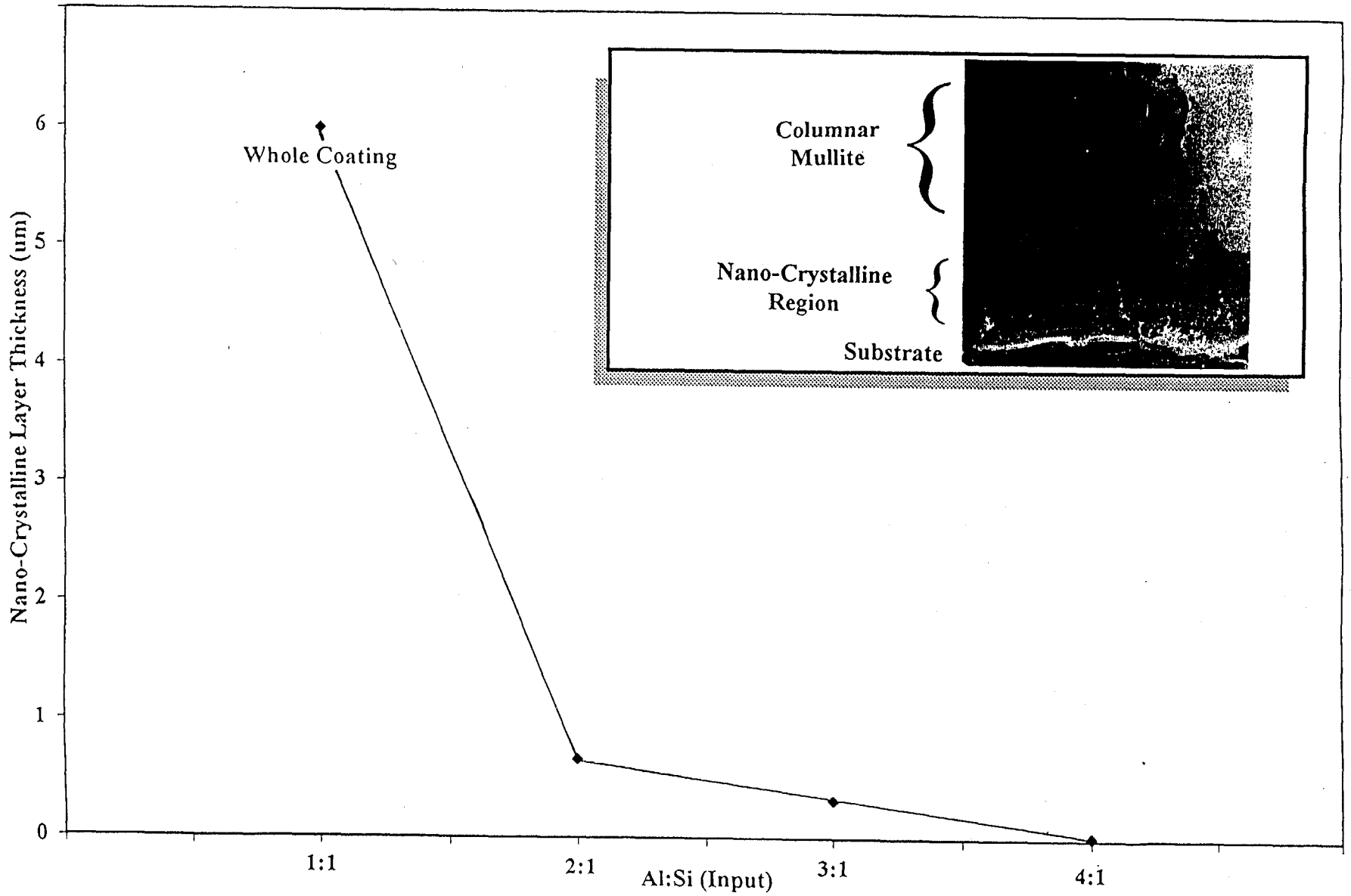

Figure 2: Nano-crystalline layer thickness of mullite coatings vs. reactant Al:Si ratio. Inset is the typical microstructural evolution of mullite coatings on silicon-based materials.

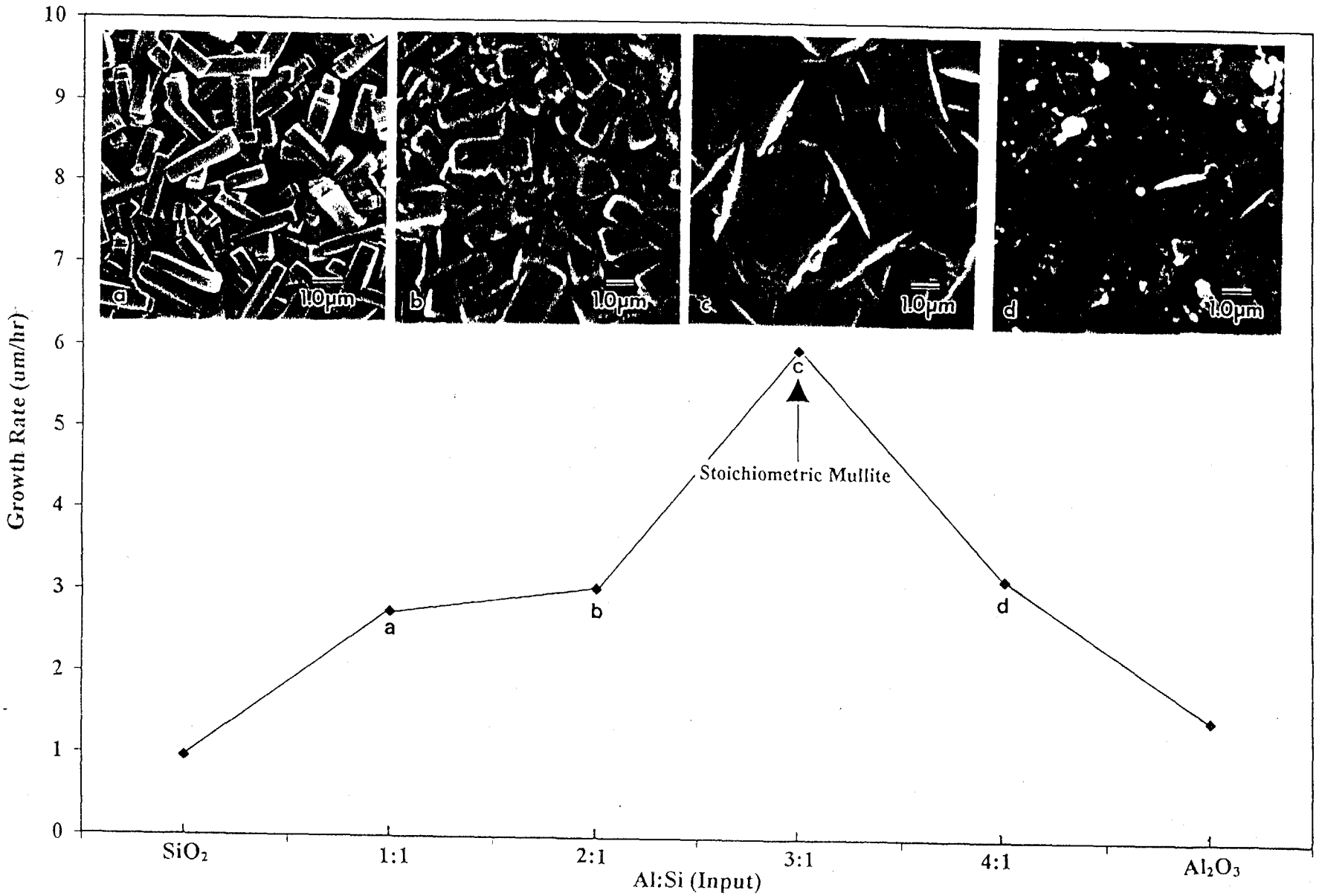

Figure 3: Growth rate of mullite vs. reactant Al:Si ratio at a constant metallic chloride partial pressure (P_{MCl_x}) of 0.53 torr.

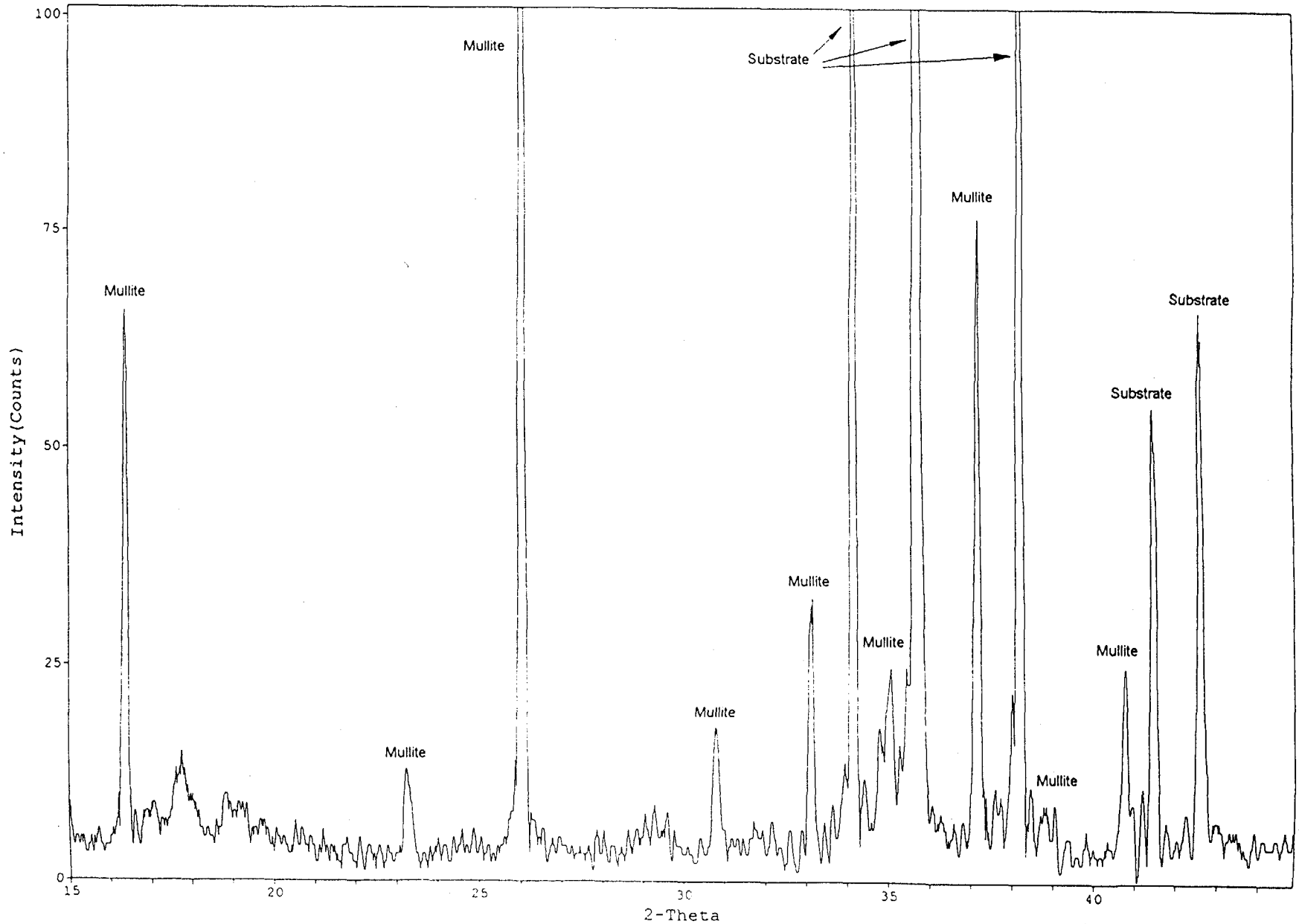

Figure 4: X-ray diffraction pattern of mullite on SiC deposited at 950°C, 75 torr, Al:Si reactant ratio of 3:1, and P_{MCl_x} of 0.53 torr.

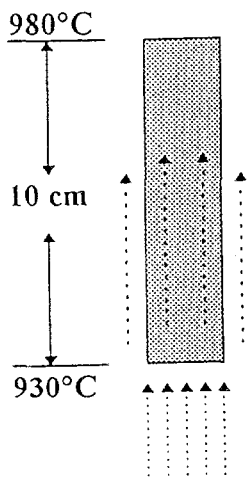

EDS Surface Analysis
Al:Si of Mullite Surface

980°C →

4:1

960°C →

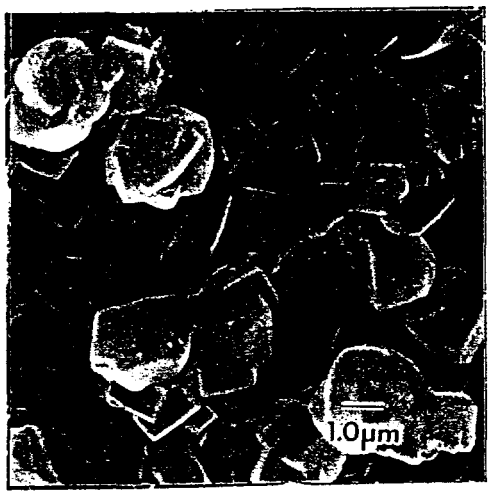

3:1

940°C →

1.4:1

930°C →

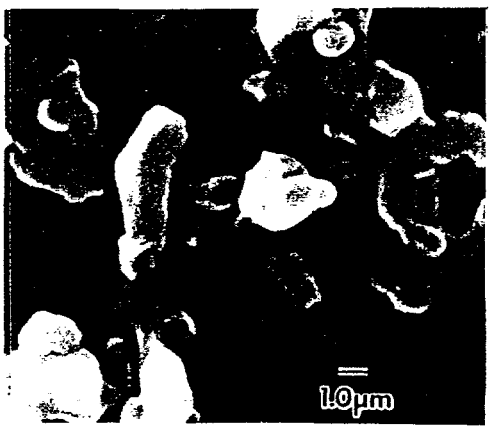

Regions of SiO_2

Figure 5: Difference in surface structure and chemical composition of mullite grown on Si_3N_4 where the sample is placed parallel to reactant gas flow.

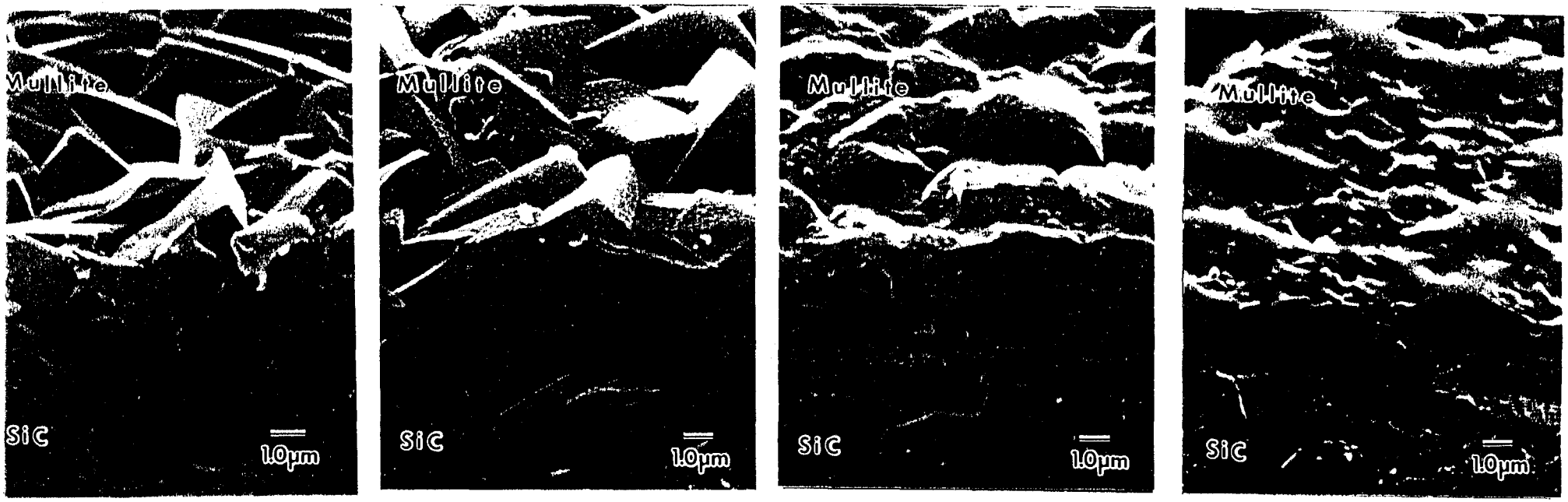

As Grown 1000°C 1200°C 1350°C

Figure 6: Surface structure of mullite as deposited, annealed in Ar @ 1000°C for 100 hours, annealed @ 1200°C for 100 hours, and 1350°C for 4 hours.

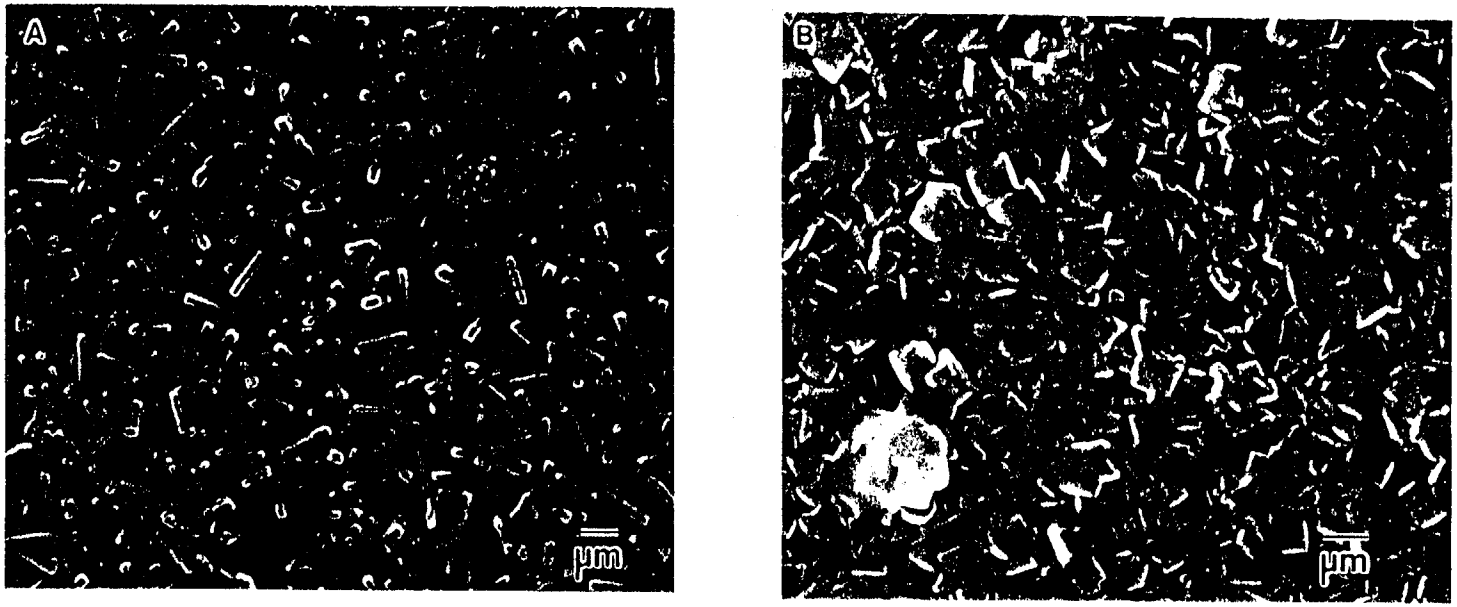

Figure 7: Surface structure of mullite after annealing in Ar @ 1350°C for 4 hours for coatings grown with an Al:Si input ratio of A) 2:1, B) 4:1.

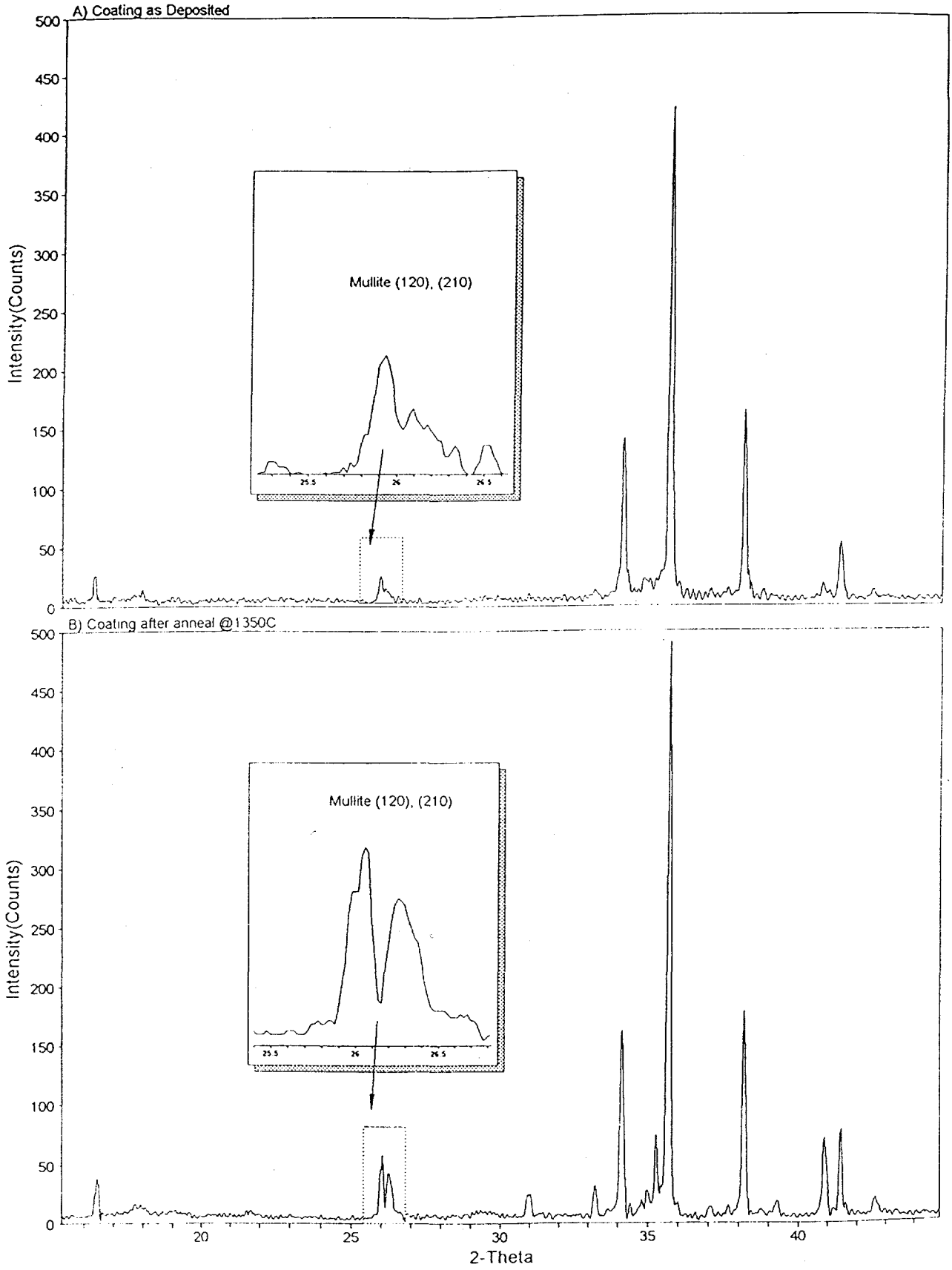

Figure 8: X-ray diffraction pattern for a mullite coating A) As Deposited, B) After annealing in Ar @ 1350°C for 4 hours.

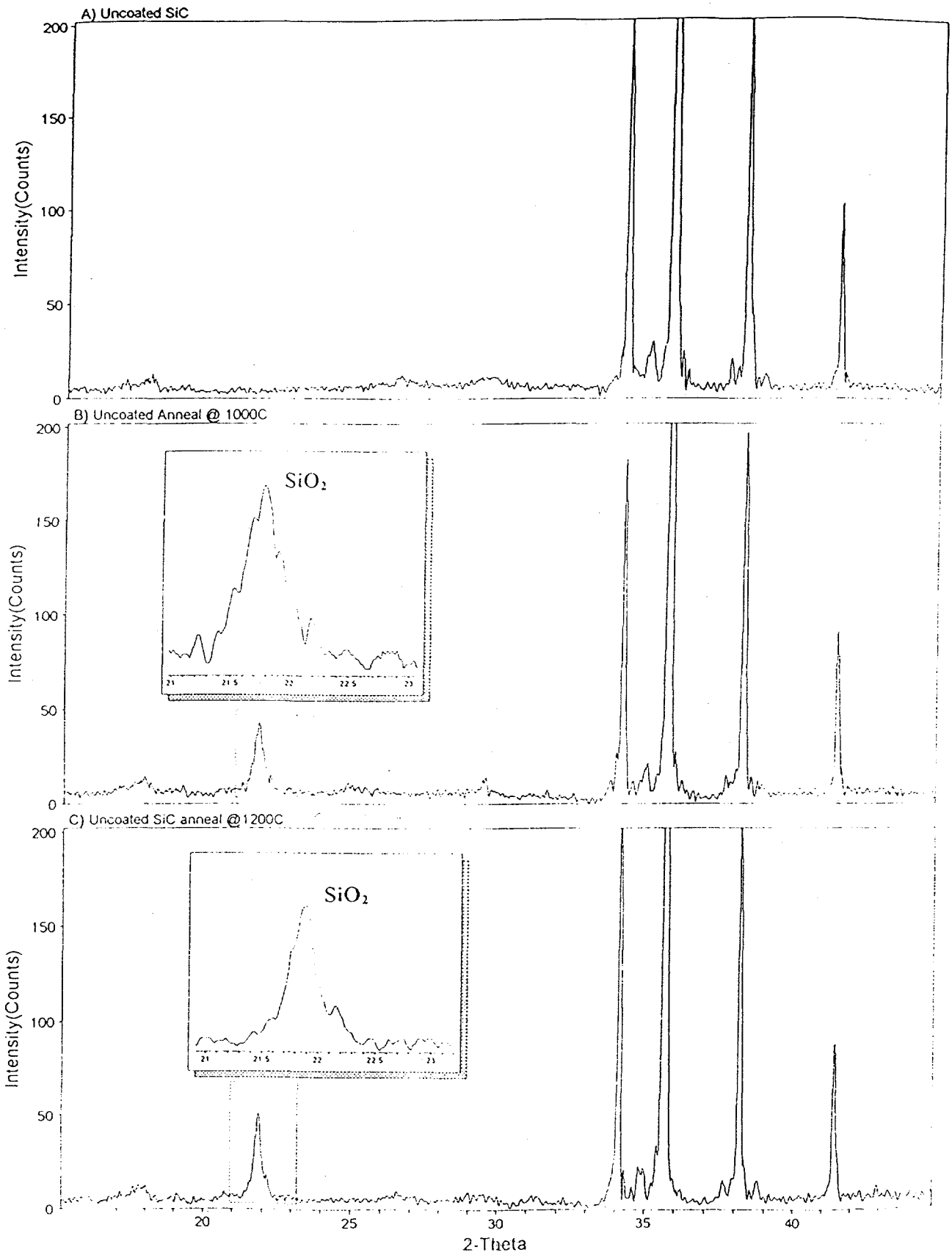

Figure 9: X-ray diffraction patterns for uncoated SiC, A) As deposited, B) Heat treated in Ar @ 1000°C for 100 hours, C) @1200°C for 100 hours.

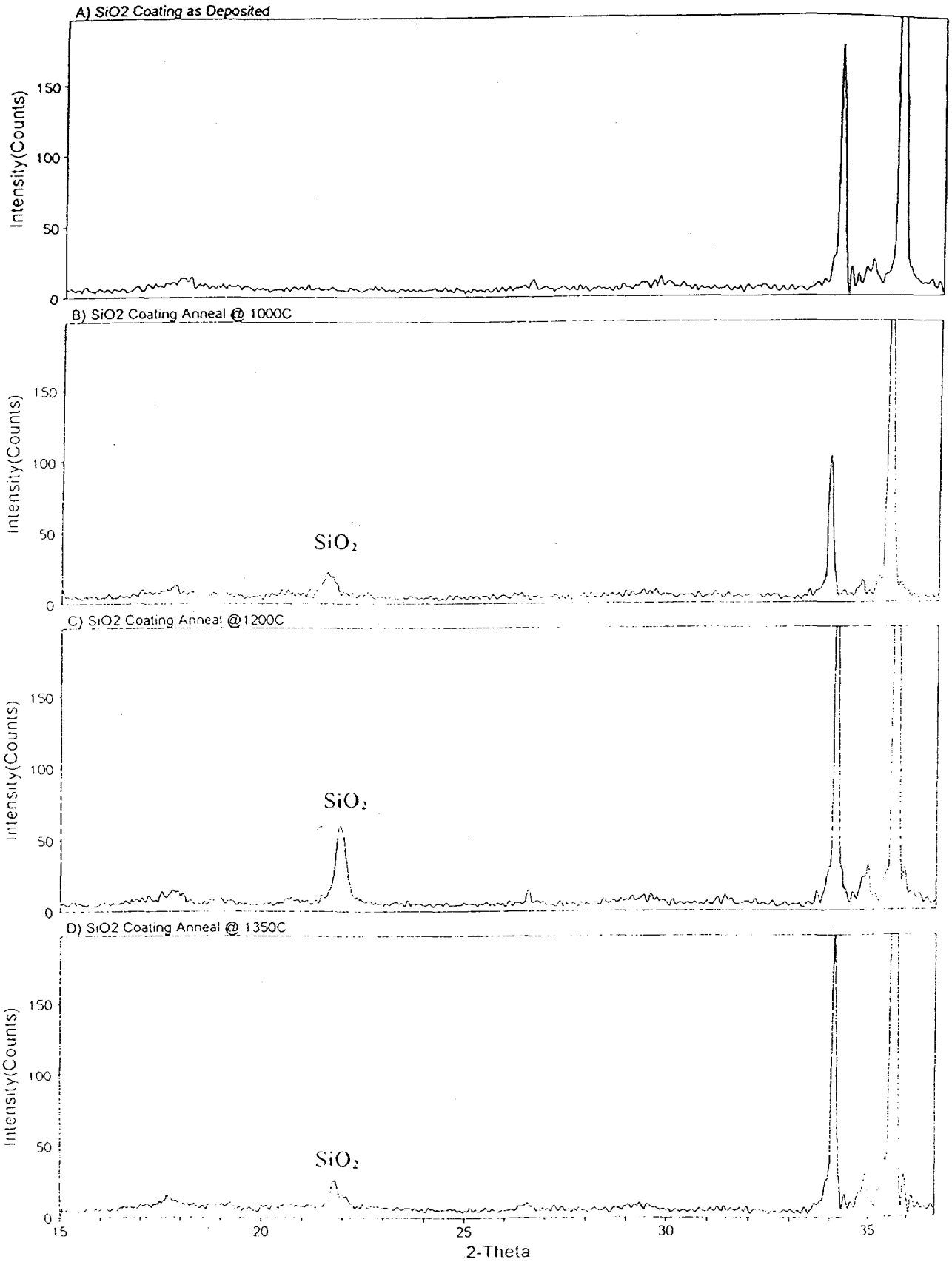

Figure 10:X-ray diffraction patterns for SiO_2 coated SiC, A) As deposited, B) Heat treated in Ar @ 1000°C for 100 hours, C) @1200°C for 100 hours, D) @1350°C for 4

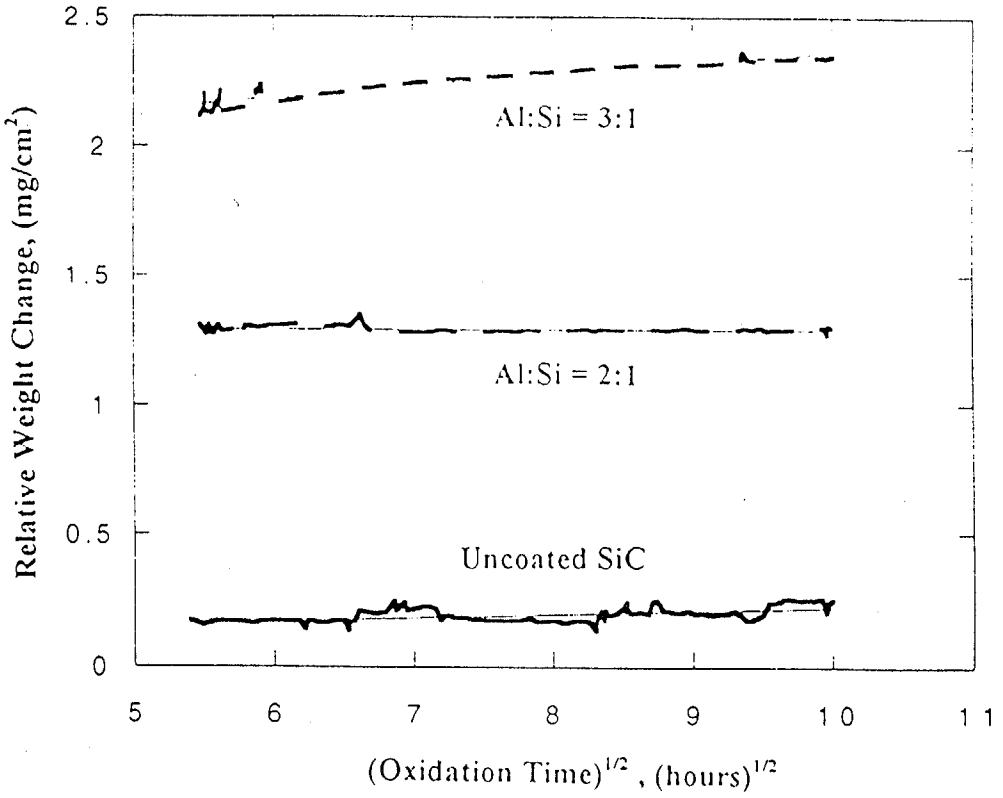

Figure 11: Relative weight change of uncoated SiC and mullite coatings grown at reactant Al:Si ratios of 2:1 and 3:1 on SiC vs. (oxidation time)$^{1/2}$ in a flowing air environment @ 1000°C. [Tortorelli Ref. 25]

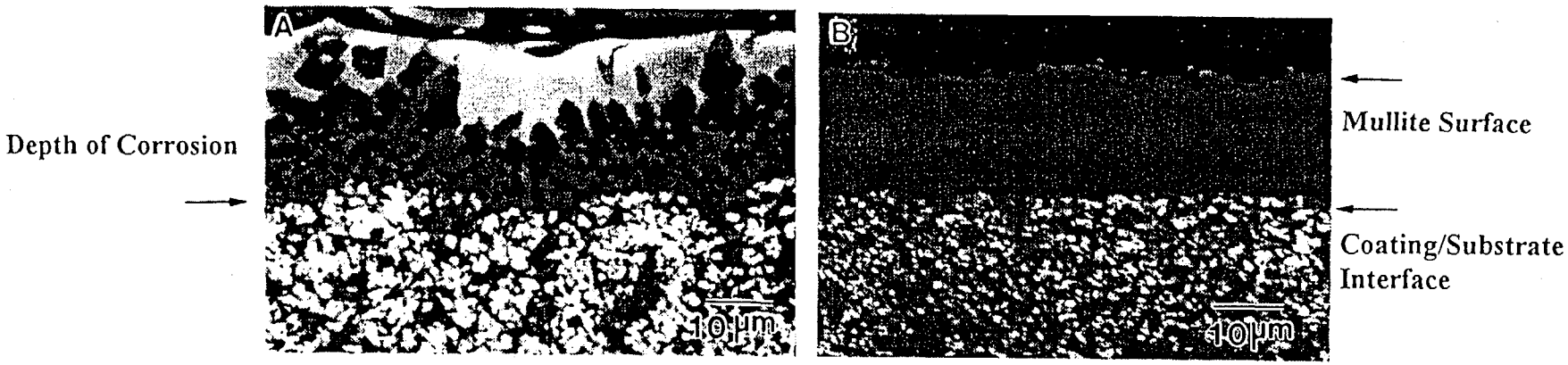

Figure 12: Comparison between, A) Uncoated Si_3N_4 and B) Mullite coated Si_3N_4 subjected to a Na_2SO_4-O_2 environment at 1000°C. White areas on the material surface are the result of corrosion.[Woo Lee Ref. 26]

Oxide	wt %
SiO_2	53.4
Al_2O_3	18.6
Fe_2O_3	17.6
TiO_2	0.7
P_2O_5	0.0
CaO	7.1
MgO	0.9
Na_2O	0.0
K_2O	1.7
SO_3	0.0

Table I: Chemical composition of coal slag which resulted from coal burned at Illinois Power Company Baldwin Plant. Commonly referred to as Baldwin coal slag. [Breder, Ref. 27]

Al:Si (Input Ratio)	Observations
2:1	Very Clean, no pitting observed
3:1	Clean, possible beginning of pit formation
4:1	Clean, possible beginning of pit formation
Uncoated SiC	Corrosion beginning

Table II: Observations of mullite grown with different input Al:Si ratios on SiC and exposed to Baldwin coal slag for 300 hours at 1260°C. [Breder, Ref. 27]

CERAMIC COMPOSITES DISTRIBUTION

3M COMPANY
Ceramic Materials Department
201-4N-01 3M Center,
St. Paul, MN 55144
M. A. Leitheiser

AIR PRODUCTS AND CHEMICALS
P.O. Box 538
Allentown, PA 18105
S. W. Dean

ALLISON GAS TURBINE DIVISION
P.O. Box 420
Indianapolis, IN 46206-0420
P. Khandelwal (Speed Code W-5)
R. A. Wenglarz (Speed Code W-16)

AMA RESEARCH & DEVELOPMENT CENTER
5950 McIntyre Street
Golden, CO 80403
T. B. Cox

ARGONNE NATIONAL LABORATORY
9700 S. Cass Avenue
Argonne, IL 60439
W. A. Ellingson
J. P. Singh

BABCOCK & WILCOX
Domestic Fossil Operations
20 South Van Buren Avenue
Barberton, OH 44023
M. Gold

BRITISH COAL CORPORATION
Coal Technology Development Division
Stoke Orchard, Cheltenham
Glocestershire, England GL52 4ZG
J. Oakey

CANADA CENTER FOR MINERAL & ENERGY TECHNOLOGY
568 Booth Street
Ottawa, Ontario
Canada K1A OG1
R. Winston Revic
Mahi Sahoo

DOE
DOE OAK RIDGE OPERATIONS
P.O.Box 2001
Oak Ridge, TN 37831
Assistant Manager for
Energy Research and Development

DOE
DOE OAK RIDGE OPERATIONS
P. O. Box 2008
Building 4500N, MS 6269
Oak Ridge, TN 37831
M. H. Rawlins

DOE
OFFICE OF BASIC ENERGY SCIENCES
Materials Sciences Division
ER-131
19901 Germantown Road
Germantown, MD 20874-1290
H. M. Kerch

DOE
IDAHO OPERATIONS OFFICE
P. O. Box 1625
Idaho Falls, ID 83415
J. B. Malmo

DOE
MORGANTOWN ENERGY TECHNOLOGY CENTER
P.O. Box 880
Morgantown, WV 26505
R. C. Bedick
D. C. Cicero
F. W. Crouse, Jr.
R. A. Dennis
N. T. Holcombe
W. J. Huber
T. J. McMahon
J. E. Notestein

DOE
OFFICE OF FOSSIL ENERGY
FE-72
19901 Germantown Road
Germantown, MD 20874-1290
F. M. Glaser

DOE
OFFICE OF VEHICLE AND ENERGY R&D
CE-151 Forrestal Building
Washington, DC 20585
R. B. Schulz

DOE
PITTSBURGH ENERGY TECHNOLOGY CENTER
P.O. Box 10940
Pittsburgh, PA 15236
A. L. Baldwin
G. V. McGurl
L. A. Ruth
T. M. Torkos

DOW CORNING CORPORATION
3901 S. Saginaw Road
Midland, MI 48686-0995
H. Atwell

EC TECHNOLOGIES
3614 Highpoint Drive
San Antonio, TX 78217
D. J. Kenton

ELECTRIC POWER RESEARCH INSTITUTE
P.O. Box 10412
3412 Hillview Avenue
Palo Alto, CA 94303
W. T. Bakker
J. Stringer

EUROPEAN COMMUNITIES JOINT RESEARCH CENTRE
Petten Establishment
P.O. Box 2
1755 ZG Petten
The Netherlands
M. Van de Voorde

GEORGIA INSTITUTE OF TECHNOLOGY
Materials Science & Engineering (0245)
Bunger-Henry Building, Room 276
Atlanta, GA 30332-0245
T. L. Starr

IDAHO NATIONAL ENGINEERING LABORATORY
P. O. Box 1625
Idaho Falls, ID 83415
B. H. Rabin

LAWRENCE LIVERMORE NATIONAL LABORATORY
P.O. Box 808, L-325
Livermore, CA 94550
W. A. Steele

NATIONAL MATERIALS ADVISORY BOARD
National Research Council
2101 Constitution Avenue
Washington, DC 20418
K. M. Zwilsky

OAK RIDGE NATIONAL LABORATORY
P.O. Box 2008
Oak Ridge, TN 37831
P. T. Carlson
F. D. Johnson **(5 copies)**
R. R. Judkins
D. P. Stinton
M. R. Upton

OFFICE OF NAVAL RESEARCH
Code 431, 800 N. Quincy Street
Arlington, VA 22217
S. G. Fishman

SHELL DEVELOPMENT COMPANY
WTC R-1371
P.O. Box 1380
Houston, TX 77251-1380
W. C. Fort

TENNESSEE VALLEY AUTHORITY
Energy Demonstration & Technology
MR2N58A
Chattanooga, TN 37402-2801
C. M. Huang

THE JOHNS HOPKINS UNIVERSITY
Materials Science & Engineering
Maryland Hall
Baltimore, MD 21218
R. E. Green, Jr.

THE MATERIALS PROPERTIES COUNCIL, INC.
United Engineering Center
345 E. Forty-Seventh Street
New York, NY 10017
M. Prager

THE NORTON COMPANY
High Performance Ceramics Division
Goddard Road
Northborough, MA 01532-1545
N. Corbin

THE TORRINGTON COMPANY
Advanced Technology Center
59 Field St.
Torrington, CT 06790
W. J. Chmura

UNION CARBIDE CORPORATION
Linde Division
P.O. Box 44
175 East Park Drive
Tonawanda, NY 14151-0044
Harry Cheung

UNITED TECHNOLOGIES RESEARCH CENTER
MS 24, Silver Lane
East Hartford, CT 06108
K. M. Prewo

UNIVERSITY OF TENNESSEE
Dept of Materials Science and Engineering
Knoxville, TN 37996-2200
Peter Liaw

UNIVERSITY OF WASHINGTON
Department of Materials Science and Engineering
101 Wilson, FB-10
Seattle, WA 98195
T. G. Stoebe

VIRGINIA POLYTECHNIC INSTITUTE & STATE UNIVERSITY
Department of Materials Engineering
Blackburg, VA 24601
K. L. Reifsnider

WESTERN RESEARCH INSTITUTE
365 N. 9th Street
P.O. Box 3395
University Station
Laramie, WY 82071
V. K. Sethi

WESTINGHOUSE ELECTRIC CORPORATION
Research and Development Center
1310 Beulah Road
Pittsburgh, PA 15235
S. C. Singhal